

1 **CYP4CL2 confers metabolic resistance to pyridaben in the citrus pest**
2 **mite *Panonychus citri***

3 Deng Pan^{a,b}, Menghao Xia^{a,b}, Chuanzhen Li^{a,b}, XunYan Liu^{a,b}, Lewis
4 Archdeacon^c, Andrias O. O'Reilly^c, Guorui Yuan^{a,b}, Jinjun Wang^{a,b}, Wei Dou^{a,b*}

5

6 ^aKey Laboratory of Entomology and Pest Control Engineering, College of Plant
7 Protection, Southwest University, Chongqing, 400715, China

8 ^bKey Laboratory of Agricultural Biosafety and Green Production of Upper Yan
9 gtze River (Ministry of Education), Academy of Agricultural Sciences,
10 Southwest University, Chongqing, 400715, China

11 ^cSchool of Biological and Environmental Sciences, Liverpool John Moores
12 University, Liverpool, L3 5UX, UK

13

14 Deng Pan: pandeng94@email.swu.edu.cn

15 Meng-Hao Xia: xiamhao@163.com

16 Lewis Archdeacon: L.R.Archdeacon@ljmu.ac.uk

17 Andrias O. O'Reilly: a.o.oreilly@ljmu.ac.uk

18 Xun-Yan Liu: liuxy1683@163.com

19 Chuan-Zhen Li: CLlblank@163.com

20 Guo-Rui Yuan: ygr@swu.edu.cn

21 Jin-Jun Wang: wangjinjun@swu.edu.cn

22 Wei Dou: douwei80@swu.edu.cn

23 *Corresponding author: Wei Dou, Key Laboratory of Entomology and Pest
24 Control Engineering, College of Plant Protection, Southwest University,
25 Chongqing 400715, China.

26 **Abstract**

27 The citrus red mite *Panonychus citri* has developed strong resistance to
28 acaricides. Cytochrome P450 monooxygenases (P450s) can detoxify
29 pesticides, and are involved in pesticide resistance in many insects. Here, a
30 pyridaben-resistant *P. citri* strain showed cross-resistance to cyenopyrafen,
31 bifenazate, fenpyroximate, and tolfenpyrad. Piperonyl butoxide, a P450 inhibitor,
32 significantly increased the toxicity of pyridaben to resistant (Pyr_Rs) and
33 susceptible (Pyr_Control) *P. citri* strains. P450 activity was significantly higher
34 in Pyr_Rs than in Pyr_Control. Analyses of RNA-Seq data identified a P450
35 gene (*CYP4CL2*) potentially involved in pyridaben resistance. Consistently, it
36 was up-regulated in two field-derived resistant populations (CQ_WZ and
37 CQ_TN). RNA interference-mediated knockdown of *CYP4CL2* significantly
38 decreased pyridaben resistance in *P. citri*. Transgenic *Drosophila melanogaster*
39 expressing *CYP4CL2* showed increased pyridaben resistance. Molecular
40 docking analysis showed that pyridaben could bind to several amino acids at
41 substrate recognition sites in *CYP4CL2*. These findings shed light on P450-
42 mediated pyridaben resistance in pest mites.

43 **Key words:** Pyridaben cross-resistance, enzymatic characteristics, RNAi,
44 transgenic flies, molecular model

45 **1 Introduction**

46 Insecticide resistance is an ongoing challenge in sustainable pest management.
47 One of the molecular mechanisms implicated in insecticide resistance is
48 increased activity of metabolic enzymes that detoxify or sequester insecticides
49 before they reach their target sites. The key metabolic enzyme cytochrome
50 P450 (P450) plays a crucial role in the detoxification of various xenobiotics,
51 including insecticides.¹ Numerous studies have shown that the induced or
52 constitutive expression of P450 genes in insecticide-resistant insect strains
53 and/or in response to insecticide exposure confers insecticide resistance.¹⁻²
54 Investigations of the molecular basis of neonicotinoid resistance in whitefly,
55 *Bemisia tabaci*, revealed that several P450 genes (including *CYP6DW3*,
56 *CYP6CM1* and *CYP4C64*) are expressed at high levels in resistant strains and
57 their encoded products play pivotal roles in resistance.³⁻⁵ Another study
58 identified a cluster of nine CYP6AE subfamily genes encoding products that are
59 capable of detoxifying several xenobiotics (xanthotoxin, 2-tridecanone, and
60 indoxacarb) *in vivo*.⁶ Overexpression of *CYP6P9a* and *CYP6P9b* in *Anopheles*
61 *funestus* conferred resistance to carbamates and their encoded products were
62 demonstrated to be able to metabolize carbamates.⁷

63 Pyridaben inhibits complex I (NADH-coenzyme Q oxidoreductase) of the
64 oxidative phosphorylation pathway, thereby disrupting mitochondrial electron
65 transport.⁸ It targets the ubiquinone binding site in the nuclear-encoded PSST,
66 the 49 kDa subunit of mitochondrial complex I.⁹⁻¹⁰ PSST is the carrier of iron-

67 sulfur cluster N2, a proposed direct electron donor for ubiquinone reduction.¹¹

68 Inhibition of electron transport by pyridaben eventually causes death.

69 Because of its effectiveness against various mite species, pyridaben has
70 been used globally as an acaricide.¹² However, its extensive use has resulted
71 in strong pyridaben resistance in some mite species, and this threatens crop
72 production.¹³⁻¹⁵ Target-site mutations in various proteins are associated with
73 high or very high acaricide resistance levels in mites.¹⁶ For example, the H92R
74 and A94V point mutations located within the PSST subunit are associated with
75 strong pyridaben resistance.¹⁷⁻¹⁸ Most studies exploring the molecular basis of
76 pyridaben resistance have focused on target site mutations, while fewer have
77 focused on the detoxifying enzymes that contribute to pyridaben resistance.

78 Citrus red mite, *Panonychus citri*, is one of the major cosmopolitan citrus pest
79 mites.¹⁸ The mites feed on the leaves, branches, and even the fruits of citrus
80 species.¹⁹ The extensive use of insecticides together with the short life cycle
81 and high reproduction of this mite has promoted the development of insecticide
82 resistance in *P. citri*.²⁰⁻²¹ Monitoring revealed a high level of pyridaben
83 resistance among this mite in several citrus orchards.¹⁴ Here, we focused on a
84 pyridaben-resistant near-isogenic line of *P. citri* that was constructed in a
85 previous study.¹⁴ We analyzed the role of detoxification as a resistance
86 mechanism by detecting the activities of detoxification enzymes and conducting
87 synergism experiments. In addition, the cross-resistance to several acaricides
88 with different modes of action was determined using bioassays. Transcriptome

89 profiling was used to identify the differentially expressed genes (DEGs)
90 between pyridaben-resistant and susceptible strains. The role of *CYP4CL2*, a
91 candidate gene in the pyridaben resistance of *P. citri*, was assessed by RNA
92 interference and Gal4/UAS overexpression system in *Drosophila*. A molecular
93 model of CYP4CL2 was obtained using AlphaFold2 and molecular docking
94 analyses were performed to predict the binding mode and key amino acids. The
95 results of these analyses reveal the mechanism by which *CYP4CL2* contributes
96 to the pyridaben resistance of *P. citri*.

97 **2 Methods and materials**

98 **2.1 Mites and chemicals**

99 A relatively susceptible strain (Pyr_Control, pyridaben LC₅₀ value of 1.649
100 mg/L) and a resistant strain (Pyr_Rs, the LC₅₀ value of 1016.406 mg/L) were
101 used in this study. These strains were obtained by crossing and generational
102 screening between a laboratory susceptible strain (Lab_S) and a pyridaben-
103 resistant strain (Pyr_R).¹⁴ Both strains were maintained in an incubator at 27 ±
104 1°C, with 60 ± 5% relative humidity (RH) under a 16:8 h light/dark photoperiod.
105 Two field populations (CQ_WZ and CQ_TN, with LC₅₀ values of 186.845 and
106 160.006 mg/L, respectively, Table S1) were collected from Wanzhou and
107 Tongnan, Chongqing, China in 2023 (E107°55'37", N30°46'39"; E105°45'13",
108 N30°04'52"). The collected mites were fed on sweet orange leaves until they
109 produced offspring. Adult mites of the first generation were used for functional
110 analyses. All of the technical-grade acaricides used in functional validation

111 analyses are listed in Table S2.

112 **2.2 Bioassays**

113 Acaricide bioassays were performed as described previously.¹⁴ Briefly, 3- to 5-
114 day-old females were transferred to leaf discs cut from fresh sweet orange
115 leaves. After 2–3 h, leaf discs with mites were dipped into acaricide solutions
116 (at least five concentrations) for 5 s and then placed on wet sponges. The
117 superfluous solution on the surface of leaf discs and around the mites was
118 removed with absorbent paper. Leaf discs were dipped in blank solution (ddH₂O,
119 containing 1% acetone and 0.1% Triton X-100) as the control. After dipping, the
120 leaf discs were incubated at $27 \pm 1^\circ\text{C}$, with $60 \pm 5\%$ RH under a 16:8 h light/dark
121 photoperiod for 24 h. The mites that did not move when touched with a soft
122 brush were considered as dead. PoloPlus v.2.0 (LeOra Software 2008) was
123 used to calculate the median lethal concentration (LC₅₀) and 95% confidence
124 limits (95% CL) in the bioassays of *P. citri*.

125 **2.3 Enzyme assays**

126 *Enzyme extract preparation and protein assays*

127 Two hundred 3- to 5-day-old female adults of the Pyr_Control or Pyr_Rs strains
128 were collected for enzymatic assays. All samples were homogenized with
129 phosphate-buffered saline (PBS) (0.04 M, pH=7.4) on ice. The homogenate
130 was centrifuged at 12,000 g for 10 min at 4°C and the supernatant was collected
131 as the enzyme extract. For each strain, four biological replicates and two
132 technical replicates were analyzed.

133 *Glutathione S-transferase activity*

134 The activity of glutathione-S-transferase (GST) was determined in a reaction
135 with the substrate 1-chloro-2,4-dinitrochloroben-zene (CDNB) (Sigma-Aldrich,
136 St Louis, MO, USA). The 0.3-mL reaction mixture consisted of 100 μ L 0.6 mM
137 CDNB, 100 μ L enzyme solution, and 100 μ L 6 mM glutathione (Sigma-Aldrich).
138 For the control, PBS (0.04 M, pH=7.4) was added instead of the enzyme extract.
139 The absorbance value at 340 nm was determined every 30 s for 5 min using an
140 xMark™ microplate spectrophotometer reader (Bio-Rad, Hercules, CA, USA).
141 Each group was analyzed with four biological replicates and two technical
142 replicates.

143 *Carboxylesterase activity*

144 The activity of carboxylesterase (CarE) was determined as described by
145 Vanasperen,²² using α -naphthyl acetate (α -NA) (Sigma-Aldrich) as the
146 substrate. The substrate solution consisted of 1 mM α -NA and 0.1 mM
147 physostigmine (Dr. Ehrenstorfer GmbH, Ausburg, Germany). For the assay, 75
148 μ L enzyme solution and 100 μ L substrate solution were added to the well of a
149 96-well plate and then incubated for 10 min at 30°C. The reaction was
150 terminated by adding 25 μ L of a mixture of 5% (w/v) sodium dodecyl sulfate
151 (SDS) (Sigma-Aldrich) and 1% (w/v) fast blue B salt (Sigma-Aldrich). The
152 absorbance value of the reaction mixture was determined at 600 nm using a
153 microplate spectrophotometer reader. For each group, four biological replicates
154 and two technical replicates were analyzed.

155 *Cytochrome P450 activity*

156 Based on the method described in previous studies, an insect CYP450 ELISA
157 kit (Hengyuan Biotechnology Co., Ltd., China) was used to determine P450
158 activity.²³ According to the manufacturer's protocols, the absorbance value of
159 each sample at 450 nm was determined using a microplate spectrophotometer
160 reader and then activity was calculated from a standard curve
161 ($y=0.0292x+0.1689$). For each group, four biological replicates and two
162 technical replicates were analyzed.

163 *Synergism assays*

164 Next, we investigated the roles of detoxification enzymes in the resistance of *P.*
165 *citri* to pyridaben using detoxification enzyme inhibitors. Three inhibitors were
166 used in these analyses: the esterase-inhibitor S, S, S tributyl-
167 phosphorotrithioate (TPP, TRC, Toronto, Canada); the cytochrome P450-
168 dependent monooxygenase-inhibitor piperonylbutoxide (PBO) (Bioway Bioruler,
169 Connecticut, USA); and the glutathione-based detoxification inhibitor
170 diethylmaleate (DEM) (AbMole, Houston, USA). The final concentration of each
171 inhibitor (TPP, PBO and DEM) resulted in a maximum rate of 5% mortality of *P.*
172 *citri*. Each detoxification enzyme inhibitor was dissolved in acetone and diluted
173 to the final concentration with ddH₂O. For the assays, 30–40 female adult mites
174 were transferred onto citrus discs with a diameter of 1.5 centimeter. Then, the
175 discs with mites were dipped into the detoxification enzyme inhibitor solutions
176 and the superfluous liquid was absorbed using filter paper. All treated mites

177 were transferred to new fresh citrus leaf discs and maintained in artificial
178 incubator for 4 h. After treatments with enzyme inhibitors, the leaf discs with
179 mites were subjected to an LC₃₀ pyridaben treatment. Each analysis was
180 conducted four times. The mortality rates of mites (%) were assessed after 24
181 h. Mites exposed to ddH₂O containing the same concentration of acetone as
182 that in the treatments served as the control.

183 *Enzyme assay data analyses*

184 Significant differences in detoxification enzyme activity between Pyr_Control
185 and Pyr_Rs strains were determined by Student's *t*-test using GraphPad 8.0
186 statistical software. Student's *t*-test was also used to detect significant
187 differences in mortality between the control group and groups treated with
188 detoxification enzyme inhibitors.

189 **2.4 RNA extraction, cDNA synthesis, and quantitative real-time PCR**

190 For each group, about 100 female adult mites were collected and total RNA
191 was isolated using the MicroElute®Total RNA Kit (Omega Bio-Tek, Norcross,
192 GA, USA) following the manufacturer's protocols. The RNA concentration was
193 measured using a NanoDrop 2000 spectrophotometer (ThermoFisher Scientific,
194 Waltham, MA, USA). RNA integrity was assessed using the RNA Nano 6000
195 Assay Kit with an Agilent Bioanalyzer 2100 system (Agilent Technologies, Palo
196 Alto, CA, USA). The absorbance ratio of optical density (OD_{260/280} and
197 OD_{260/230}) was used to assess the purity of the RNA, and 1% w/v agarose
198 gel electrophoresis confirmed its integrity. All RNA samples were stored at

199 –80°C until further use. The PrimeScript RT reagent Kit (TaKaRa Biotechnology,
200 Dalian, China) was used to synthesize cDNA.

201 All primers for quantitative real-time PCR (qPCR) were designed using
202 tools at the National Center for Biotechnology Information (NCBI) PrimerBlast
203 (<http://www.ncbi.nlm.nih.gov/tools/primer-blast/>) and are listed in Table S3. The
204 10 µL qPCR reaction mixture consisted of 5 µL 2×NovoStar® SYBR qPCR
205 SuperMix Plus (Novoprotein, Shanghai, China), 3 µL cDNA, 0.5 µL each primer
206 (forward and reverse), and 1 µL RNase-free water. The PCR analyses were
207 performed on a CFX384™ Real-Time System (Bio-Rad). The thermocycling
208 conditions were as follows: 95°C for 30 s, followed by 40 cycles of 95°C for 5 s
209 and 60°C for 30 s. Gene transcript levels were standardized based on the
210 transcript levels of the reference genes *PcGAPDH* and *PcELF1A* using qBase²⁴.
211 qPCR analyses were conducted to determine the transcript levels of *CYP4CL2*
212 in different field and laboratory strains and in the *CYP4CL2*-silenced strains.
213 The experiment consisted of three treatments with three biological replicates in
214 a completely randomized design. Each replicate was analyzed with two
215 technical replicates.

216 **2.5 Transcriptome sequencing and data analysis**

217 Total RNA was extracted from 200 female adults of the Pyr_Control or Pyr_Rs
218 strains using the MicroElute®Total RNA Kit (Omega Bio-Tek), according to the
219 manufacturer's instructions. After the quality and quantity of RNA were
220 determined using a 2100 Bioanalyzer (Agilent) and a NanoDrop 2000

221 instrument (ThermoFisher Scientific), 1 µg total RNA per sample was used to
222 construct a cDNA library using the VAHTS Universal V6 RNA-seq Library Prep
223 Kit for Illumina (Vazyme, Nanjing, China). The cDNA libraries were sequenced
224 on the Illumina NovaSeq 6000 platform (Illumina Inc., San Diego, CA, USA)
225 following the protocols of the NovaSeq 6000 S4 Reagent kit (Illumina) and 150-
226 bp paired-end reads were generated. Four biological replicates were
227 sequenced for each strain.

228 To obtain clean reads, Trimmomatic (version 0.36) was used to remove the
229 low-quality reads and adaptor sequences. The remaining high-quality reads
230 were mapped to the complete *P. citri* genome (GeneBank: JAAABK000000000)
231 using HISAT2. All uniquely mapped reads were used to calculate the gene
232 RPKM (reads per kilobase of exon per million mapped sequenced reads)
233 values, which indicated the normalized gene transcript levels. The DEGs
234 between Pyr_Control and Pyr_Rs strains were selected using the bioconductor
235 package DESeq2, and met the following criteria: *P*-value < 0.05 and fold
236 change >2. Kyoto Encyclopedia of Genes and Genomes (KEGG) enrichment
237 analysis of DEGs was conducted using KOBAS software (version 2.1.1) with a
238 *P*-value < 0.05.

239 **2.6 RNA interference**

240 To explore the role of the P450 gene in the pyridaben resistance of *P. citri*, RNAi
241 was used to suppress its expression. The mites were soaked in dsRNA solution
242 as described elsewhere.²⁵ Briefly, dsRNA primers containing a T7 promoter at

243 the 5' end for the *P450* gene and GFP were designed using PrimerBlast (Table
244 S3). The dsRNA was synthesized *in vitro* using the TranscriptAid T7 High Yield
245 Transcription Kit (Thermo Fisher Scientific). Then, the quality of the dsRNA was
246 determined by 1% agarose gel electrophoresis and the concentration was
247 measured using a NanoVue UV-Vis spectrophotometer (Thermo Fisher
248 Scientific).

249 Three-day-old female mites were soaked in the dsRNA solution (1000
250 ng/ μ L) at 25°C for 24 h according to a recent study.³² The mites were
251 transferred to fresh citrus leaves and left for 4–6 h before RNA isolation and
252 pyridaben bioassays. The bioassays were conducted as described above and
253 differences between the dsRNA-treated and control groups were determined
254 by probit analysis (PoloPlus v.2.0, LeOra Software, 2008). The hypotheses of
255 equality and parallelism, and the methods used to calculate the lethal dose ratio
256 at LC₅₀ (LCR₅₀) and the 95% confidence limits (CL) were as described
257 elsewhere.²⁶

258 **2.7 Mortality bioassay of transgenic *Drosophila melanogaster***

259 The Gal4/UAS system²⁷ was used to overexpress P450 in *D. melanogaster*.
260 The open reading frames of the CYP4CL2 genes were each subcloned into
261 pJFRC28-10XUAS-IVS-GFP-p10 (Addgene Plasmid #36431). Each plasmid
262 was then microinjected into *D. melanogaster* embryos. Using the PhiC31
263 system, the plasmid DNA was integrated at the attP40 docking site on
264 chromosome 2 to generate the transgenic line, UAS-CYP4CL2. Virgin females

265 from the Act5C-GAL4 strain were crossed with males carrying UAS-CYP4CL2
266 to obtain a heritable transgenic line, Gal4/UAS-CYP4CL2. Each line was reared
267 under artificial conditions at 25°C with 60% RH under 12:12 h light/dark
268 photoperiod. The transcript level of CYP4CL2 in transgenic flies was
269 determined by qPCR, relative to that of the housekeeping gene *RPL11*²⁸ (Table
270 S3). Flies with the same background as the UAS-CYP4CL2 transgenic lines
271 were used as controls.

272 Bioassays to assess the toxicity of pyridaben to transgenic lines were
273 carried out as described previously.²⁸ Filter papers impregnated with pyridaben
274 (1000 mg/L, a lethal concentration of pyridaben) were rolled up and placed in
275 30-cc glass vials, covering the entire wall. All vials were plugged with cotton
276 soaked in 10% (w/v) sucrose. Then 25–30 flies were transferred into each vial,
277 and knockdown rate was scored after 24 h of exposure to pyridaben. For all
278 assays, five replicates were analyzed. Student's *t*-test was used to compare
279 knockdown rate of each experimental group with that of the control group.

280 **2.8 CYP4CL2 modelling and pyridaben docking**

281 To identify the amino acids within each substrate recognition site (SRS) of
282 CYP4CL2, the primary sequence was aligned with that of HaCYP6AE19²⁹
283 using Clustal Omega.³⁰ A model of the CYP4CL2 enzyme was generated using
284 AlphaFold2³¹ by submitting the primary sequence to the ColabFold website³²
285 and running AlphaFold2 with default options. The generated model lacked the
286 heme group; therefore, this co-factor was introduced into the model by copying

287 the atom coordinates of heme from a high-resolution human P450 structure as
288 described elsewhere,³³ followed by 100 steps of conjugate-gradient energy
289 minimization in SWISS-PdbViewer.³⁴

290 A 3D structure file for pyridaben (ZINC1543237) was retrieved from the
291 ZINC database (ZINC20, A Free Ultralarge-Scale Chemical Database for
292 Ligand Discovery).³⁵ Automated docking of pyridaben with the CYP4CL2 model
293 was performed by first using AutoDockTools (v1.5.7) (Molecular Graphics
294 Laboratory, Scripps Research Institute, La Jolla, CA, USA) to define rotatable
295 bonds and merge non-polar hydrogens. Then, AutoDock Vina (v1.2.3)³⁶ was
296 used to dock pyridaben within a grid of 20 × 22 × 24 points (1 Å spacing) that
297 covered the CYP4CL2 active site. The figure was produced using UCSF
298 ChimeraX version 1.5.

299 **3 Results**

300 **3.1 Cross-resistance to other pesticides in the pyridaben-resistant strain**

301 The cross-resistance of the pyridaben-resistant strain (Pyr_Rs), which shows
302 616.377-fold resistance¹⁴ compared with that of the relatively susceptible strain
303 (Pyr_Control), to ten different acaricides was determined. As shown in Table 1,
304 the 95% confidence limits of the LC₅₀ values of cyenopyrafen, bifenazate,
305 fenpyroximate, and tolfenpyrad in Pyr_Rs and Pyr_Control did not overlap,
306 indicating that there were significant differences in resistance to these
307 acaricides between Pyr_Rs and Pyr_Control.

308 The Pyr_Rs strain showed cross-resistance to fenpyroximate (63.369-fold

309 that of Pyr_Control), and low cross-resistance to cyenopyrafen, bifenazate, and
310 tolfenpyrad (3.282-fold, 4.787-fold, and 7.278-fold that of Pyr_Control,
311 respectively). There was no obvious cross-resistance to cyflumetofen,
312 abamectin, fenpropathrin, propargite, tebufenpyrad, and fenazaquin, given the
313 overlap of the 95% confidence limits of the LC₅₀ values.

314 **3.2 Detoxification enzyme activity and synergism bioassays**

315 The specific enzyme activities of CarEs, GST, and P450 are shown in Table 2.
316 The P450 activity was significantly higher in Pyr_Rs than in Pyr_Control (1.550-
317 fold higher, $P=0.006$), at 0.262 and 0.169 nmol/mg pro/min, respectively. There
318 were no significant differences in CarEs, and GST activity between Pyr_Rs and
319 Pyr_Control.

320 The results of synergism studies using the enzyme inhibitors PBO, TPP,
321 and DEM on Pyr_Rs and Pyr_Control strains are shown in Fig. 1. Pretreatment
322 with PBO significantly synergized pyridaben toxicity, with 2.613- and 1.807-fold
323 synergism in the Pyr_Rs and Pyr_Control strains, respectively. Pretreatment
324 with DEM and TPP did not significantly affect pyridaben toxicity in either Pyr_Rs
325 or Pyr_Control.

326 **3.3 Differentially expressed genes (DEGs) identification and functional** 327 **annotation**

328 In total, eight independent cDNA libraries constructed from Pyr_Rs and
329 Pyr_Control were sequenced on the Illumina sequencing platform. These
330 analyses generated a mean of 7.67 Gb clean data for each library (Table S4).

331 The Q30 value was 94.5% and the GC content ranged from 38% to 41%,
332 indicating that the quality of the data was sufficient for transcriptome analysis.
333 The raw data was uploaded to NCBI database with the biosample accessions
334 SAMN37473146-SAMN37473153.

335 To identify the potential detoxification genes involved in *P. citri* pyridaben
336 resistance, we detected DEGs between Pyr_Rs and Pyr_Control strains (Fig.
337 2). In total, there were 204 DEGs with an absolute fold-change of ≥ 2 and *P*-
338 value (FDR) < 0.05 . Of these, 91 genes were significantly up-regulated and 113
339 were down-regulated in Pyr_Rs *versus* Pyr_Control (Fig. 2A). To identify the
340 function of the up-regulated genes, they were annotated at the KEGG
341 database. Most of them were attributed to metabolic pathways, especially the
342 drug metabolism pathway (Fig. 2B). This result suggested that genes in the
343 drug metabolism pathway may be involved in pyridaben metabolism in the
344 pyridaben-resistant *P. citri* strain.

345 Based on the up-regulated genes from comparative transcriptomics
346 between Pyr_Rs and Pyr_Control strains, one p450 gene and three ABC
347 transporter genes were identified (Table S5). The previous synergism analyses
348 indicated that P450s contributed to pyridaben resistance in *P. citri*. Therefore,
349 the P450 gene, EVM0004731(*CYP4CL2*), was considered as a candidate gene
350 involved in resistance to pyridaben. Subsequently, gene function analysis were
351 performed *in vivo* and *in vitro*.

352 **3.4 Functional analysis of *CYP4CL2***

353 The qPCR results showed that *CYP4CL2* was significantly up-regulated in the
354 pyridaben-resistant *P. citri* strains (Pyr_R and Pyr_Rs) and two resistant field
355 populations (CQ_WZ and CQ_TN) (Fig. 3), as compared with the susceptible
356 strains Lab_S and Pyr_Control. We generated RNAi lines by feeding mites with
357 a dsRNA solution to suppress the expression of *CYP4CL2*. The transcript levels
358 of *CYP4CL2* and the silencing efficiency in different *P. citri* strain/populations
359 were confirmed by qPCR (dsCYP4CL2 significantly reduced *CYP4CL2*
360 expression as compared to dsGFP.) (Fig. S1). As the 95% CL of LCR₅₀ >1, the
361 tests for the hypotheses of equality revealed significant differences in the LC₅₀
362 values to pyridaben among test groups (Table 3).³³ Consequently, the LC₅₀
363 values were significantly reduced in all test strain/populations with silenced or
364 low *CYP4CL2* expression (the LC₅₀ values were reduced from 2.535 to 1.185
365 mg/L, 1276.617 to 637.595 mg/L, 174.709 to 91.028 mg/L, and 215.237 to
366 93.766 mg/L in the RNAi-treated Pyr_Control, Pyr_Rs, CQ_TN, and CQ_WZ,
367 respectively) (Table 3). These results suggest that *CYP4CL2* has played an
368 important role in the development of pyridaben resistance in *P. citri*.

369 To determine whether *CYP4CL2* confers cross-resistance, we evaluated
370 the susceptibility of *CYP4CL2*-silenced lines to bifenazate, fenpyroximate, and
371 tolfenpyrad (Fig. S2). No obvious differences in susceptibility were observed
372 between *CYP4CL2*-silenced lines and the controls, indicating that *CYP4CL2*
373 did not participate in cross-resistance to bifenazate, fenpyroximate, and
374 tolfenpyrad (Fig. S2).

375 **3.5 Pyridaben resistance of *Drosophila melanogaster* overexpressing**
376 **CYP4CL2**

377 Next, we determined whether expression of CYP4CL2 alone was sufficient to
378 confer pyridaben resistance *in vivo*. For these analyses, CYP4CL2 was
379 overexpressed in transgenic *D. melanogaster* using the Gal4/UAS system. We
380 constructed UAS-CYP4CL2 and Gal4/UAS-CYP4CL2 transgenic flies. The
381 results of qPCR analyses confirmed that CYP4CL2 was overexpressed in the
382 Gal4/UAS-CYP4CL2 line, but not in the control lines (UAS-CYP4CL2) (Fig. 4A).
383 The knockdown rate of flies treated with a lethal concentration (1000mg/L) of
384 pyridaben were recorded to determine their resistance to pyridaben. Bioassays
385 carried out with pyridaben on the transgenic Gal4/UAS-CYP4CL2 line indicated
386 significantly increased resistance in this line (Fig. 4B), with a significantly lower
387 knockdown rate (68.2% after 24 h; $P < 0.001$) than that of the control line (94.4%
388 for UAS-CYP4CL2).

389 **3.6 Molecular modeling and pyridaben docking analysis**

390 The SRSs of CYP4CL2 were identified using the sequence of another P450
391 (HaCYP6AE19)²⁹ as reference (Fig. S3). A model of CYP4CL2 was then
392 generated to determine if pyridaben could be accommodated within its active
393 site. Fig. 5 shows the top-scoring docking prediction (estimated free energy of
394 binding (ΔG_b) of -4.115 kcal/mol), which placed pyridaben in proximity to the
395 heme group. This docking position allowed pyridaben to have possible binding
396 interactions with amino acid side chains from four of the six SRSs (SRS1, 4, 5,

397 and 6). Because none of these amino acids were predicted to form a hydrogen
398 bond with the ligand, van der Waals interactions were predicted to be the main
399 type of ligand-binding interaction.

400 **Discussion**

401 Insecticides are powerful weapons in the control of insect pests that threaten
402 crop production. Whilst maintaining the efficacy of these insecticides and the
403 integrity of their targets is vital, the evolution of insecticide resistance in target
404 pests due to strong selection pressure imposed by widespread insecticide use
405 is a serious problem.³⁷ In addition, cross-resistance to compounds in the same
406 insecticide group is a frequently observed phenomenon. Cross-resistance
407 among groups of insecticides that differ in their structural and functional
408 characteristics can be extremely unpredictable in the field. Many studies have
409 focused on cross-resistance between pyridaben and other acaricides in
410 different spider mites. For example, fenpyroximate-resistant strains selected in
411 the laboratory showed moderate level of cross-resistance to pyridaben.³⁸ In
412 *Tetranychus cinnabarinus* (Boisduval), *CYP389C16* directly contributes to the
413 cross-resistance between cyflumetofen and pyridaben by hydroxylation.³⁹
414 Another study selected for cyenopyrafen resistance in *Tetranychus urticae*, and
415 bioassay results confirmed the development of cross-resistance to pyridaben.⁴⁰
416 Similarly, the development of resistance to bifenazate in *T. urticae* was found to
417 be accompanied by cross-resistance to pyridaben and other acaricides.⁴¹ In the
418 current study, the *P. citri* pyridaben-resistant strain exhibited cross-resistance

419 to several tested acaricides (cyenopyrafen, bifenazate, fenpyroximate, and
420 tolfenpyrad), consistent with the results of the studies mentioned above.

421 The *P. citri* pyridaben-resistant strain showed higher P450 activity
422 compared with that of the susceptible strain. Moreover, the toxicity of pyridaben
423 to the resistant and susceptible strains of *P. citri* was significantly increased by
424 PBO (a known inhibitor of P450), suggesting that P450 may be involved in the
425 detoxification of pyridaben. This result was in accordance with the results of a
426 previous study on pyridaben-selected *T. urticae* strains.¹⁵ Overexpression of
427 their respective genes was found to be the cause of increased enzyme activities
428 in resistant strains. In general, genetic phenomena are responsible for
429 resistance to metabolic-based insecticides.¹ Genomic changes lead to the
430 amplification, overexpression, and variations in the coding sequences of major
431 groups of genes encoding metabolic enzymes. Of these, P450s play critical
432 roles in the development of resistance to synthetic insecticides.⁴² In insects, the
433 induction and constitutive overexpression of genes encoding P450s are
434 responsible for the detoxification of insecticides.⁴³ A large number of insect
435 P450s involved in insecticide resistance have been identified and functionally
436 analyzed. Based on the DEGs detected from the RNA-seq data, *CYP4CL2* was
437 identified as a potentially important gene in detoxification in our study.
438 Consistent with this, a previous study reported that this P450 gene was
439 significantly up-regulated in *P. citri* exposed to sublethal concentration of
440 pyridaben.⁴⁴ We also detected up-regulation of *CYP4CL2* in different resistant

441 populations, providing further evidence for its important role in the development
442 of pyridaben resistance in *P. citri*.

443 To confirm the function of P450 in pyridaben resistance, we performed
444 gene-silencing using the RNAi method. When the expression of *CYP4CL2* was
445 suppressed by dsRNA delivery, the resistance of *P. citri* significantly decreased
446 both in laboratory strains and field populations. These RNAi results
447 demonstrate the importance of *CYP4CL2* in pyridaben resistance. The
448 knockdown of *CYP4CL2* did not affect the responses of *P. citri* to LC₃₀
449 treatments with bifenazate, fenpyroximate, and tolfenpyrad, indicating that this
450 P450 gene was not responsible for the cross-resistance against these
451 acaricides, even though it confers resistance to pyridaben.

452 The transgenic *Drosophila* system for *in vivo* gene expression has proved
453 to be powerful tool for exploring the genetic basis of insecticide resistance over
454 the last 60 years.⁴⁵ Transgenic overexpression of P450s in *D. melanogaster*
455 using the Gal4/UAS system has been used successfully to evaluate the function
456 of many P450 genes from different insects. For example, transgenic *D.*
457 *melanogaster* overexpressing the *Plutella xylostella* (L.) *CYP6BG1* gene
458 showed significantly increased tolerance to chlorantraniliprole.⁴⁶ Similarly,
459 *NICYP6CS1* was introduced into *D. melanogaster* to clarify its contribution to
460 pymetrozine resistance in *Nilaparvata lugens*.⁴⁷ Transgenic *D. melanogaster*
461 overexpressing two *N. lugens* P450 genes (*CYP6ER1vA* and *CYP439A1*)
462 exhibited significant resistance to buprofezin.⁴⁸ Another study reported that the

463 duplication and divergence of *CYP6ER1* in *N. lugens* has led to resistance to
464 several neonicotinoids.³³ The transgenic flies have been frequently applied in
465 P450 function analysis when the active recombinant protein can't be
466 achieved,⁴⁶⁻⁴⁸ which could provide evidence in P450 mediated resistance
467 development in combination with the RNAi assay. Therefore, we introduced
468 *CYP4CL2* into *Drosophila* to verify the function *in vitro*. Here, overexpression
469 of the *P. citri* P450 gene *CYP4CL2* in *D. melanogaster* significantly increased
470 its pyridaben resistance. These results provide further evidence that the up-
471 regulation of *CYP4CL2* plays an important role in pyridaben resistance in *P. citri*.

472 P450 proteins share a conserved protein fold with six highly variable SRSs
473 that frame the catalytic pocket and substrate access channels, and this
474 variability contributes to the catalytic specificity of the enzyme.⁴⁹ Site-directed
475 mutagenesis studies have shown that SRSs constitute several important
476 domains of the tertiary structure of P450 proteins and contribute to their
477 function.⁵⁰ The P450 catalytic site is mainly formed by SRS1, SRS4, SRS5, and
478 SRS6 and the substrate access channel is shaped mainly by SRS2 and
479 SRS3.⁵¹ Although mutations both within and outside³⁶ SRS regions can confer
480 insecticide resistance by increasing ligand affinity or active-site accessibility for
481 a substrate. In addition, our transgenic *Drosophila* study shows that *P. citri*
482 *CYP4CL2* significantly promotes the tolerance of fly to pyridaben. An increase
483 in *CYP4CL2* expression therefore appears to be the prevalent mechanism in
484 current populations of resistant *P. citri*. We predict that there may be selective

485 pressure for the *CYP4CL2* gene to duplicate further boosts its activity towards
486 pyridaben to increase resistance.

487 In summary, our bioassay results provide evidence of cross-resistance
488 between pyridaben and other acaricides in a pyridaben-resistant strain of *P. citri*.
489 Enzyme activity and synergism analyses suggested that P450s contribute to
490 pyridaben resistance. Analyses of RNA-Seq data revealed an up-regulated
491 P450 gene, *CYP4CL2*, in a pyridaben-resistant strain of *P. citri*. Expression
492 analyses revealed the up-regulation of *CYP4CL2* in several different resistant
493 strains/populations. RNAi-mediated knockdown of this P450 gene increased
494 the susceptibility of *P. citri* to pyridaben, whereas transgenic *D. melanogaster*
495 expressing *CYP4CL2* showed significantly increased pyridaben resistance.
496 Molecular modelling indicated the pyridaben could be accommodated within the
497 *CYP4CL2* active site. These results provide useful information about the
498 mechanism of P450-mediated resistance to pyridaben in *P. citri* and identify the
499 *CYP4CL2* gene as an important target for future genetic screening of resistant
500 *P. citri* populations.

501

502

503 **Acknowledgements**

504 We thank Yuchuang Li for helping to collect mites. This study was supported by
505 the Science and Technology Basic Resources Investigation Program of China
506 (2018FY101105), the Fundamental Research Funds for the Central
507 Universities (SWU-XDPY22001, SWU-XJLJ202304) of China, the China

508 Agricultural Research System of MOA and MARA, and the Medical Research
509 Council (MRC) [grant number MR/W002159/1].

510 **Notes**

511 The authors declare no competing financial interest.

512 **References**

- 513 1. Li, X.; Schuler, M. A.; Berenbaum, M. R., Molecular mechanisms of metabolic resistance
514 to synthetic and natural xenobiotics. *Annu. Rev. Entomol.* **2007**, *52* (1), 231-253.
- 515 2. Daborn, P. J.; Yen, J. L.; Bogwitz, M. R.; Le Goff, G.; Feil, E.; Jeffers, S.; Tijet, N.; Perry, T.;
516 Heckel, D.; Batterham, P.; Feyereisen, R.; Wilson, T. G.; ffrench-Constant, R. H., A single P450
517 allele associated with insecticide resistance in *Drosophila*. *Science* **2002**, *297* (5590), 2253-
518 2256.
- 519 3. Yang, X.; Wei, X. G.; Yang, J.; Du, T. H.; Yin, C.; Fu, B.; Huang, M. J.; Liang, J. J.; Gong, P.
520 P.; Liu, S. N.; Xie, W.; Guo, Z. J.; Wang, S. L.; Wu, Q. J.; Nauen, R.; Zhou, X. G.; Bass, C.;
521 Zhang, Y. J., Epitranscriptomic regulation of insecticide resistance. *Sci. Adv.* **2021**, *7* (19),
522 eabe5903.
- 523 4. Yang, X.; Deng, S.; Wei, X. G.; Yang, J.; Zhao, Q. N.; Yin, C.; Du, T. H.; Guo, Z. J.; Xia, J.
524 X.; Yang, Z. Z.; Xie, W.; Wang, S. L.; Wu, Q. J.; Yang, F. S.; Zhou, X. G.; Nauen, R.; Bass, C.;
525 Zhang, Y. J., MAPK-directed activation of the whitefly transcription factor *CREB* leads to P450-
526 mediated imidacloprid resistance. *Proc. Natl. Acad. Sci. U. S. A.* **2020**, *117* (19), 10246-10253.
- 527 5. Xue, H.; Fu, B.; Huang, M. J.; He, C.; Liang, J. J.; Yang, J.; Wei, X. G.; Liu, S. N.; Du, T.
528 H.; Ji, Y.; Yin, C.; Gong, P. P.; Hu, J. Y.; Du, H.; Zhang, R.; Wang, C.; Khajehali, J.; Su, Q.; Yang,
529 X.; Zhang, Y. J., CYP6DW3 metabolizes imidacloprid to imidacloprid-urea in whitefly (*Bemisia*
530 *tabaci*). *J. Agric. Food Chem.* **2023**, *71* (5), 2333-2343.
- 531 6. Wang, H. D.; Shi, Y.; Wang, L.; Liu, S.; Wu, S. W.; Yang, Y. H.; Feyereisen, R.; Wu, Y. D.,
532 CYP6AE gene cluster knockout in *Helicoverpa armigera* reveals role in detoxification of
533 phytochemicals and insecticides. *Nature Commun.* **2018**, *9* (1), 4820.

- 534 7. Mugenzi, L. M. J.; Tekoh, T. A.; Ibrahim, S. S.; Muhammad, A.; Kouamo, M.; Wondji, M. J.;
535 Irving, H.; Hearn, J.; Wondji, C. S., The duplicated P450s CYP6P9a/b drive carbamates and
536 pyrethroids cross-resistance in the major African malaria vector *Anopheles funestus*. *Plos*
537 *Genet.* **2023**, *19* (3). e1010678.
- 538 8. Yaghoobi, R.; Khajehali, J.; Alavijeh, E. S.; Nauen, R.; Dermauw, W.; Van Leeuwen, T.,
539 Fenpyroximate resistance in Iranian populations of the European red mite *Panonychus ulmi*
540 (Acari: Tetranychidae). *Exp. Appl. Acarol.* **2021**, *83* (1), 69-79.
- 541 9. Fiedorczuk, K.; Letts, J. A.; Degliesposti, G.; Kaszuba, K.; Skehel, M.; Sazanov, L. A.,
542 Atomic structure of the entire mammalian mitochondrial complex I. *Nature* **2016**, *538* (7625),
543 406-410.
- 544 10. Zickermann, V.; Wirth, C.; Nasiri, H.; Siegmund, K.; Schwalbe, H.; Hunte, C.; Brandt, U.,
545 Mechanistic insight from the crystal structure of mitochondrial complex I. *Science* **2015**, *347*
546 (6217), 44-49.
- 547 11. Duarte, M.; Populo, H.; Videira, A.; Friedrich, T.; Schulte, U., Disruption of iron-sulphur
548 cluster N2 from NADH: ubiquinone oxidoreductase by site-directed mutagenesis. *Biochem. J.*
549 **2002**, *364* (3), 833-839.
- 550 12. Devine, G. J.; Barber, M.; Denholm, I., Incidence and inheritance of resistance to METI-
551 acaricides in European strains of the two-spotted spider mite (*Tetranychus urticae*) (Acari:
552 Tetranychidae). *Pest. Manag. Sci.* **2001**, *57* (5), 443-448.
- 553 13. Koo, H. N.; Choi, J.; Shin, E.; Kang, W.; Cho, S. R.; Kim, H.; Park, B.; Kim, G. H.,
554 Susceptibility to acaricides and the frequencies of point mutations in etoxazole- and pyridaben-
555 resistant strains and field populations of the two-spotted spider mite, *Tetranychus urticae* (Acari:

556 Tetranychidae). *Insects*. **2021**, *12* (7), 660.

557 14. Pan, D.; Xia, M. H.; Luo, Q. J.; Liu, X. Y.; Li, C. Z.; Yuan, G. R.; Wang, J. J.; Dou, W.,
558 Resistance of *Panonychus citri* (McGregor) (Acari: Tetranychidae) to pyridaben in China:
559 monitoring and fitness costs. *Pest Manag. Sci.* **2023**, *79* (3), 996-1004.

560 15. Namin, H. H.; Zhurov, V.; Spenler, J.; Grbic, M.; Grbic, V.; Scott, I. M., Resistance to
561 pyridaben in Canadian greenhouse populations of two-spotted spider mites, *Tetranychus*
562 *urticae* (Koch). *Pestic. Biochem. Physiol.* **2020**, *170*.

563 16. Ilias, A.; Vontas, J.; Tsagkarakou, A., Global distribution and origin of target site insecticide
564 resistance mutations in *Tetranychus urticae*. *Insect Biochem. Mol. Biol.* **2014**, *48*, 17-28.

565 17. Snoeck, S.; Kurlovs, A. H.; Bajda, S.; Feyereisen, R.; Greenhalgh, R.; Villacis-Perez, E.;
566 Kosterlitz, O.; Dermauw, W.; Clark, R. M.; Van Leeuwen, T., High-resolution QTL mapping in
567 *Tetranychus urticae* reveals acaricide-specific responses and common target-site resistance
568 after selection by different METI-I acaricides. *Insect Biochem. Mol. Biol.* **2019**, *110*, 19-33.

569 18. Alavijeh, E. S.; Khajehali, J.; Snoeck, S.; Panteleri, R.; Ghadamyari, M.; Jonckheere, W.;
570 Bajda, S.; Saalwaechter, C.; Geibel, S.; Douris, V.; Vontas, J.; Van Leeuwen, T.; Dermauw, W.,
571 Molecular and genetic analysis of resistance to METI-I acaricides in Iranian populations of the
572 citrus red mite, *Panonychus citri*. *Pestic. Biochem. Physiol.* **2020**, *164*, 73-84.

573 19. Jones, V. P.; Parrella, M. P., The sublethal effects of insecticides on life table parameters
574 of *Panonychus citri* (Acari: Tetranychidae). *Can. Entomol.* **1984**, *116* (7), 1033-1040.

575 20. Ran, C.; Chen, Y.; Wang, J. J., Susceptibility and carboxylesterase activity of five field
576 populations of *Panonychus citri* (McGregor) (Acari: Tetranychidae) to four acaricides. *Int. J.*
577 *Acarol.* **2009**, *35* (2), 115-121.

- 578 21. Pan, D.; Luo, Q. J.; O'Reilly, A. O.; Yuan, G.R.; Wang, J. J.; Dou, W., Mutations of voltage-
579 gated sodium channel contribute to pyrethroid resistance in *Panonychus citri*. *Insect Sci.* **2023**.
580 <https://doi.org/10.1111/1744-7917.13266>.
- 581 22. Van Asperen, K., A study of housefly esterases by means of a sensitive colorimetric
582 method. *J. Insect Physiol.* **1962**, 8 (4), 401-416.
- 583 23. Wang, L.; Cui, L.; Wang, Q. Q.; Chang, Y. P.; Huang, W. L.; Rui, C. H., Sulfoxaflor
584 resistance in *Aphis gossypii*: resistance mechanism, feeding behavior and life history changes.
585 *J. Pest Sci.* **2022**, 95 (2), 811-825.
- 586 24. Hellemans, J.; Mortier, G.; De Paepe, A.; Speleman, F.; Vandesompele, J., qBase relative
587 quantification framework and software for management and automated analysis of real-time
588 quantitative PCR data. *Genome Biol.* **2007**, 8 (2), R19.
- 589 25. Sun, Q. Z.; Li, X. L.; Shi, Y. F.; Zhang, Y. C.; Chai, W. J.; Chen, R. Y.; Niu, J.; Wang, J. J.,
590 GARP: A family of glycine and alanine-rich proteins that helps spider mites feed on plants.
591 *Insect Sci.* **2022**, 0, 1–15
- 592 26. He, Y.; Zhang, J.; Chen, J., Effect of synergists on susceptibility to chlorantraniliprole in
593 field populations of *Chilo suppressalis* (Lepidoptera: Pyralidae). *J. Econ. Entomol.* **2014**, 107
594 (2), 791-796.
- 595 27. Pfeiffer, B. D.; Truman, J. W.; Rubin, G. M., Using translational enhancers to increase
596 transgene expression in *Drosophila*. *Proc. Natl. Acad. Sci. U. S. A.* **2012**, 109 (17), 6626-6631.
- 597 28. Riveron, J. M.; Irving, H.; Ndula, M.; Barnes, K. G.; Ibrahim, S. S.; Paine, M. J. I.; Wondji,
598 C. S., Directionally selected cytochrome P450 alleles are driving the spread of pyrethroid
599 resistance in the major malaria vector *Anopheles funestus*. *Proc. Natl. Acad. Sci. U. S. A.*

600 **2013**, *110* (1), 252-257.

601 29. Shi, Y.; Sun, S.; Zhang, Y. J.; He, Y. S.; Du, M. H.; ÓReilly, A. O.; Wu, S. W.; Yang, Y. H.;
602 Wu, Y. D., Single amino acid variations drive functional divergence of cytochrome P450s in
603 *Helicoverpa* species. *Insect Biochem. Mol. Biol.* **2022**, *146*, 103796.

604 30. Sievers, F.; Wilm, A.; Dineen, D.; Gibson, T. J.; Karplus, K.; Li, W.; Lopez, R.; McWilliam,
605 H.; Remmert, M.; Söding, J.; Thompson, J. D.; Higgins, D. G., Fast, scalable generation of high-
606 quality protein multiple sequence alignments using Clustal Omega. *Mol. Syst. Biol.* **2011**, *7* (1),
607 539.

608 31. Jumper, J.; Evans, R.; Pritzel, A.; Green, T.; Figurnov, M.; Ronneberger, O.;
609 Tunyasuvunakool, K.; Bates, R.; Žídek, A.; Potapenko, A.; Bridgland, A.; Meyer, C.; Kohl, S. A.
610 A.; Ballard, A. J.; Cowie, A.; Romera-Paredes, B.; Nikolov, S.; Jain, R.; Adler, J.; Back, T.;
611 Petersen, S.; Reiman, D.; Clancy, E.; Zielinski, M.; Steinegger, M.; Pacholska, M.; Berghammer,
612 T.; Bodenstein, S.; Silver, D.; Vinyals, O.; Senior, A. W.; Kavukcuoglu, K.; Kohli, P.; Hassabis,
613 D., Highly accurate protein structure prediction with AlphaFold. *Nature* **2021**, *596* (7873), 583-
614 589.

615 32. Mirdita, M.; Schütze, K.; Moriwaki, Y.; Heo, L.; Ovchinnikov, S.; Steinegger, M., ColabFold:
616 making protein folding accessible to all. *Nature Methods* **2022**, *19* (6), 679-682.

617 33. Duarte, A.; Pym, A.; Garrood, W. T.; Troczka, B. J.; Zimmer, C. T.; Davies, T. G. E.; Nauen,
618 R.; O'Reilly, A. O.; Bass, C., P450 gene duplication and divergence led to the evolution of dual
619 novel functions and insecticide cross-resistance in the brown planthopper *Nilaparvata lugens*.
620 *Plos Genet.* **2022**, *18* (6), e1010279.

621 34. Guex, N.; Diemand, A.; Peitsch, M. C., Protein modelling for all. *Trends Biochem. Sci.* **1999**,

622 24 (9), 364-367.

623 35. Irwin, J. J.; Tang, K. G.; Young, J.; Dandarchuluun, C.; Wong, B. R.; Khurelbaatar, M.;
624 Moroz, Y. S.; Mayfield, J.; Sayle, R. A., ZINC20—A free ultralarge-scale chemical database for
625 ligand discovery. *J. Chem. Inf. Model.* **2020**, *60* (12), 6065-6073.

626 36. Trott, O.; Olson, A. J., AutoDock Vina: Improving the speed and accuracy of docking with
627 a new scoring function, efficient optimization, and multithreading. *J. Comput. Chem.* **2010**, *31*
628 (2), 455-461.

629 37. Perry, T.; Batterham, P.; Daborn, P. J., The biology of insecticidal activity and resistance.
630 *Insect Biochem. Mol. Biol.* **2011**, *41* (7), 411-422.

631 38. Kim, Y. J.; Lee, S. H.; Lee, S. W.; Ahn, Y. J., Fenpyroximate resistance in *Tetranychus*
632 *urticae* (Acari : Tetranychidae): cross-resistance and biochemical resistance mechanisms. *Pest*
633 *Manag.t Sci.* **2004**, *60* (10), 1001-1006.

634 39. Feng, K. Y.; Ou, S. Y.; Zhang, P.; Wen, X.; Shi, L.; Yang, Y. W.; Hu, Y.; Zhang, Y. C.; Shen,
635 G. M.; Xu, Z. F.; He, L., The cytochrome P450 *CYP389C16* contributes to the cross-resistance
636 between cyflumetofen and pyridaben in *Tetranychus cinnabarinus* (Boisduval). *Pest Manag.*
637 *Sci.* **2020**, *76* (2), 665-675.

638 40. Khalighi, M.; Dermauw, W.; Wybouw, N.; Bajda, S.; Osakabe, M.; Tirry, L.; Van Leeuwen,
639 T., Molecular analysis of cyenopyrafen resistance in the two-spotted spider mite *Tetranychus*
640 *urticae*. *Pest Manag. Sci.* **2016**, *72* (1), 103-112.

641 41. Kim, E.; Ahn, K. S.; Gil-Hah, K.; 유정수; 서동규; 한종빈, Inheritance and cross resistance
642 of bifenazate resistance in two-spotted spider mite, *Tetranychus urticae*. *Korean J. Appl.*
643 *Entomol.* **2005**, *44* (2), 151-156.

644 42. Feyereisen, R., Insect CYP genes and P450 enzymes. *Insect Mol. Biol. Biochem.* **2012**;
645 236-316.

646 43. Liu, N.; Li, M.; Gong, Y.; Liu, F.; Li, T., Cytochrome P450s – their expression, regulation,
647 and role in insecticide resistance. *Pestic. Biochem. Physiol.* **2015**, *120*, 77-81.

648 44. Ding, T. B.; Niu, J. Z.; Yang, L. H.; Zhang, K.; Dou, W.; Wang, J. J., Transcription profiling
649 of two cytochrome P450 genes potentially involved in acaricide metabolism in citrus red mite
650 *Panonychus citri*. *Pestic. Biochem. Physiol.* **2013**, *106* (1-2), 28-37.

651 45. Perry, T.; Batterham, P., Harnessing model organisms to study insecticide resistance. *Curr.*
652 *Opin. Insect Sci.* **2018**, *27*, 61-67.

653 46. Li, X. X.; Li, R.; Zhu, B.; Gao, X. W.; Liang, P., Overexpression of cytochrome P450
654 *CYP6BG1* may contribute to chlorantraniliprole resistance in *Plutella xylostella* (L.). *Pest Manag.*
655 *Sci.* **2018**, *74* (6), 1386-1393.

656 47. Wang, L. X.; Tao, S.; Zhang, Y.; Jia, Y. L.; Wu, S. F.; Gao, C. F., Mechanism of metabolic
657 resistance to pymetrozine in *Nilaparvata lugens*: over-expression of cytochrome P450
658 *CYP6CS1* confers pymetrozine resistance. *Pest Manag. Sci.* **2021**, *77* (9), 4128-4137.

659 48. Zeng, B.; Liu, Y. T.; Feng, Z. R.; Chen, F. R.; Wu, S. F.; Bass, C.; Gao, C. F., The
660 overexpression of cytochrome P450 genes confers buprofezin resistance in the brown
661 planthopper, *Nilaparvata lugens* (Stål). *Pest Manag. Sci.* **2023**, *79* (1), 125-133.

662 49. Guengerich, F. P.; Waterman, M. R.; Egli, M., Recent structural insights into cytochrome
663 P450 function. *Trends. Pharmacol. Sci.* **2016**, *37* (8), 625-640.

664 50. Pan, L.; Wen, Z.; Baudry, J.; Berenbaum, M. R.; Schuler, M. A., Identification of variable
665 amino acids in the SRS1 region of CYP6B1 modulating furanocoumarin metabolism. *Arch.*

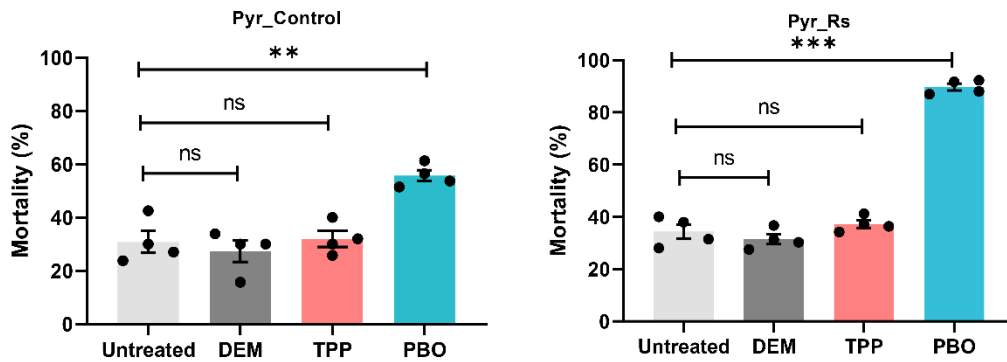
666 *Biochem. Biophys.* **2004**, 422 (1), 31-41.

667 51. Schuler, M. A.; Berenbaum, M. R., Structure and function of cytochrome P450S in insect

668 adaptation to natural and synthetic toxins: insights gained from molecular modeling. *J. Chem.*

669 *Ecol.* **2013**, 39 (9), 1232-1245.

670



671

672 **Fig. 1. Susceptibility of Pyr_Control and Pyr_Rs strains to LC₃₀ pyridaben**

673 **after treatment with three enzyme inhibitors.** Data are means ± S.E.M.

674 Asterisks indicate statistically significant difference: ***: $P < 0.001$, ns indicates

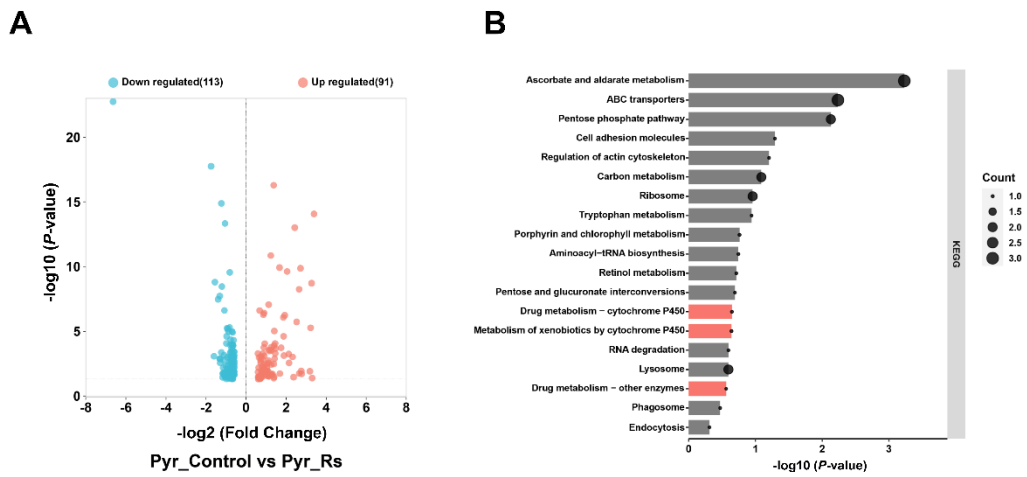
675 no significance. Four dots mean four biological replicates in each condition.

676 DEM refers to diethyl maleate; TPP refers to S, S, S tributyl-phosphorotrithioate;

677 PBO refers to piperonylbutoxide.

678

679



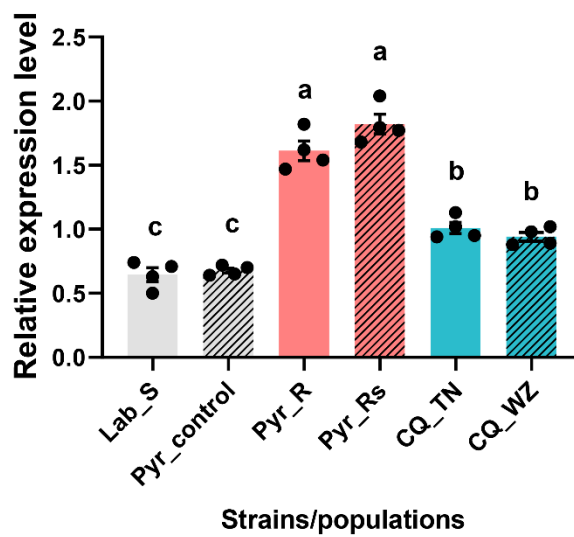
680

681 **Fig. 2. Comparative transcriptome analysis between Pyr_Control and**

682 **Pyr_Rs strains. A.** Differentially expressed genes between Pyr_Control and

683 Pyr_Rs strains. **B.** KEGG pathway function annotation of up-regulated genes.

684



685

686 **Fig. 3. Transcript levels of *CYP4CL2* in different strains/populations.** Data

687 are means ± S.E.M. Different letters indicated a significant difference among

688 strains/populations. (ANOVA, Tukey, $P < 0.05$). Four dots mean four biological

689 replicates in each strain or population. Lab_S, the susceptible strain was raised

690 in lab from 2016. Pyr_R, a pyridaben-resistant population collected from a citrus

691 orchard at Nanning, Guangxi Province, China in 2019. Pyr_Control and Pyr_Rs,

692 two laboratory strains were recombination inbred lines obtained from

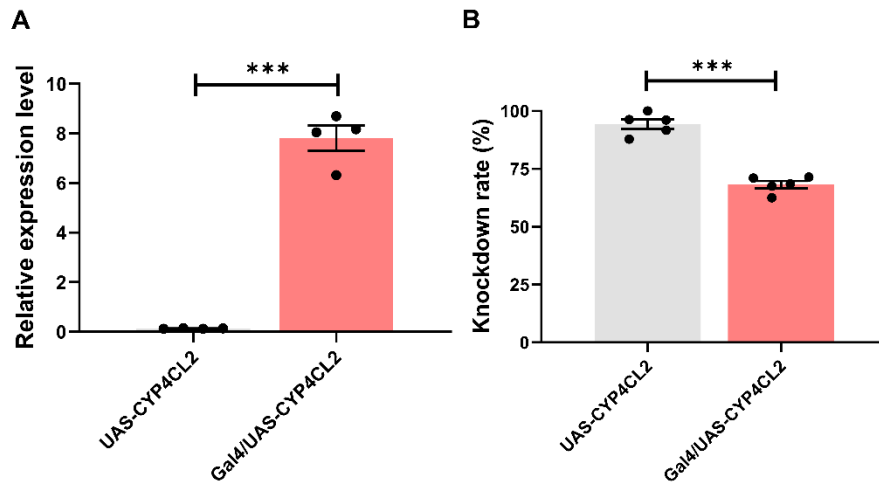
693 hybridization between Lab_S and Pyr_R within pyridaben selection. CQ_TN

694 and CQ_WZ, two field populations were collected from citrus orchards in

695 Tongnan, Chongqing municipality and Wanzhou, Chongqing municipality.

696

697



698

699 **Fig. 4. Transcript levels of *CYP4CL2* in transgenic *Drosophila***

700 ***melanogaster* and pyridaben resistance of transgenic lines. A.** Relative

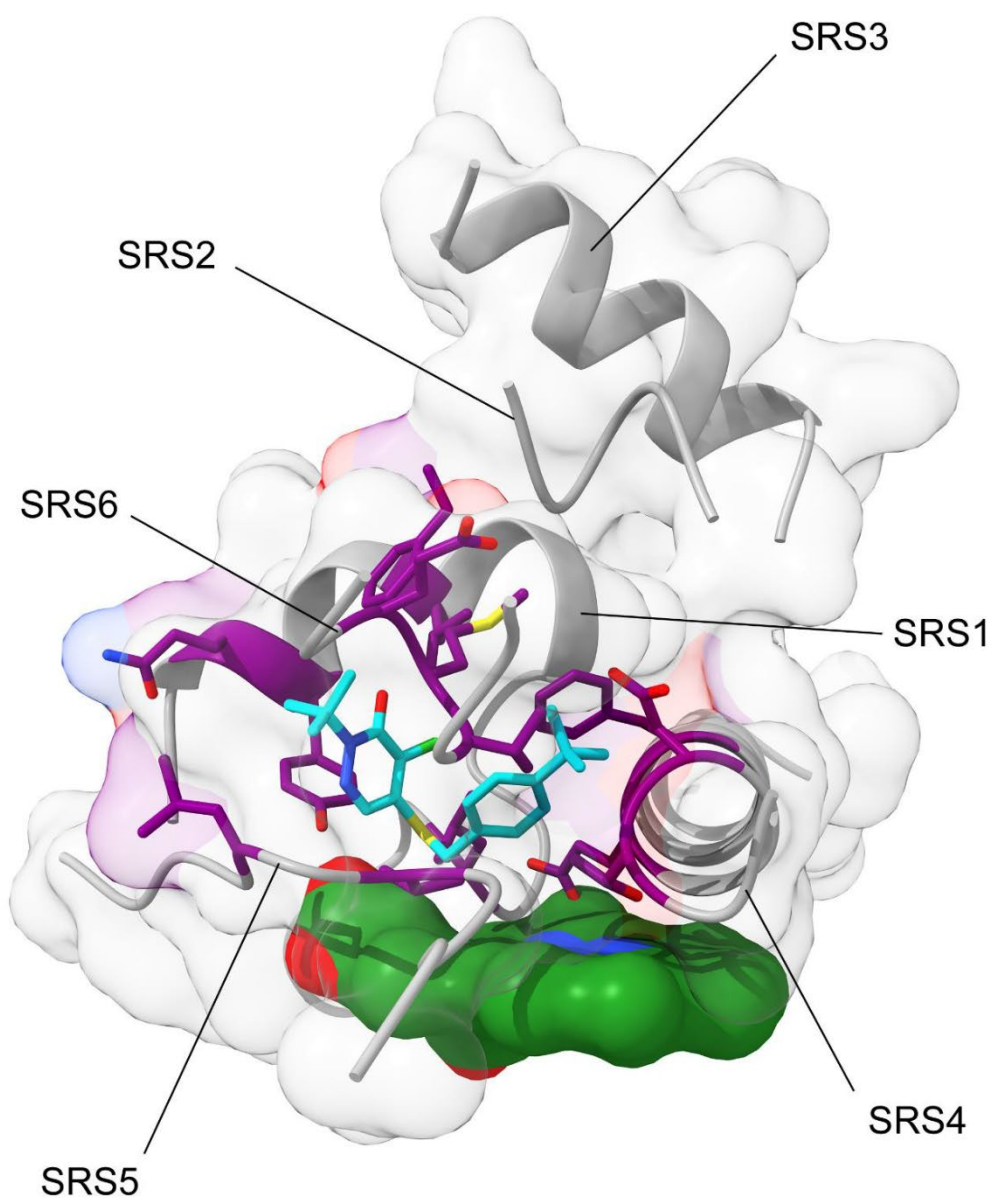
701 transcript levels of *CYP4CL2* in UAS-CYP4CL2 and Gal4/UAS-CYP4CL2 lines.

702 **B.** Mortality of transgenic lines after treatment with pyridaben. UAS-CYP4CL2

703 dots are shown on light grey bar and Gal4/UAS-CYP4CL2 dots are shown on

704 pink bar. Data are means \pm S.E.M. Asterisks indicate significant difference (**):

705 $P < 0.001$). Four dots mean four biological replicates in each line.



706

707 **Fig. 5. Docking prediction for pyridaben in an Alphafold2-generated**

708 **CYP4CL2 model.** SRS1–6 regions surrounding the active site of CYP4CL2 are

709 shown as ribbons with semi-transparent surfaces. Heme co-factor is shown in

710 green space-fill and pyridaben is shown as cyan sticks. Amino acids <math>< 4.0 \text{ \AA}</math>

711 from docked pyridaben are shown as purple sticks.

712

Table 1. Bioassays of different acaricides with various modes of action against Pyr_Control and Pyr_Rs strains.

Groups	Acaricides	Strain	N	Slope (\pm SE)	LC ₅₀ (mg/L)95%CL ^a	χ^2 (df)	RRs ^b
Mitochondrial complex II electron transport inhibitors	Cyflumetofen	Pyr_control	426	1.546 \pm 0.164	6.917 (3.863 – 18.216)	13.972 (4)	1
		Pyr_Rs	440	1.601 \pm 0.157	5.926 (3.404 – 12.566)	14.573 (4)	0.857
	Cyenopyrafen	Pyr_control	509	2.356 \pm 0.189	0.560 (0.479 – 0.649)	4.473 (5)	1
		Pyr_Rs	571	2.225 \pm 0.183	1.838 (1.575 – 2.130)	2.178 (4)	3.282
Glutamate-gated chloride channel (GluCl) allosteric modulators	Abamectin	Pyr_control	334	1.248 \pm 0.117	0.032 (0.006 – 0.081)	19.772 (4)	1
		Pyr_Rs	764	1.718 \pm 0.164	0.077 (0.052 – 0.116)	7.625 (4)	2.406
Sodium channel modulators	Fenpropathrin	Pyr_control	507	4.053 \pm 0.419	27.508 (22.478 – 33.181)	4.480 (4)	1
		Pyr_Rs	390	2.041 \pm 0.199	35.511 (29.669 – 43.286)	3.167 (4)	1.291
Inhibitors of mitochondrial ATP synthase	Propargite	Pyr_control	433	1.474 \pm 0.150	40.131 (32.599 – 50.304)	0.167 (4)	1
		Pyr_Rs	454	1.438 \pm 0.165	79.161 (48.178 – 186.089)	9.680 (4)	1.973
Mitochondrial complex III electron transport inhibitors – Qo site	Bifenazate	Pyr_control	501	1.860 \pm 0.166	28.468 (20.344 – 38.450)	5.596 (4)	1
		Pyr_Rs	569	2.098 \pm 0.191	136.275 (105.658 – 174.956)	5.437 (4)	4.787
Mitochondrial	Fenpyroximate	Pyr_control	637	1.904 \pm 0.153	14.889 (11.216 – 18.932)	4.764 (4)	1

complex I electron		Pyr_Rs	608	2.663±0.270	943.212 (639.422 – 1409.787)	15.059 (4)	63.349
transport inhibitors	Tolfenpyrad	Pyr_control	443	1.533±0.160	289.230 (187.633 – 425.892)	5.796 (4)	1
		Pyr_Rs	497	1.556±0.198	2104.924 (1313.934 – 5072.115)	10.550 (4)	7.278
	Tebufenpyrad	Pyr_control	440	2.298±0.189	145.347(114.310 – 188.029)	5.177 (4)	1
		Pyr_Rs	529	2.949±0.252	225.965(191.511 – 272.152)	5.230 (4)	1.555
	Fenazaquin	Pyr_control	520	2.263±0.203	30.894(26.389 – 36.428)	1.970 (4)	1
		Pyr_Rs	699	2.405±0.176	22.415(19.792 – 25.400)	2.998 (4)	0.726

^aCL, confidence limits.

^bRR, resistance ratio = LC₅₀ of Pyr_Rs / LC₅₀ of Pyr_control.

Table 2. CarEs, GST, and P450 activities in Pyr_Control and Pyr_Rs strains.

Detoxification enzymes	Strain	Activity of		
		detoxification enzymes	R/S	<i>P</i> -value ^a
GSTs ($\mu\text{mol/mg pro/min}$)	Pyr_control	0.233 \pm 0.018	0.910	0.130
	Pyr_Rs	0.212 \pm 0.014		
CarEs (nmol/mg pro/min)	Pyr_control	0.141 \pm 0.004	1.014	0.390
	Pyr_Rs	0.143 \pm 0.002		
P450s (nmol/mg pro/min)	Pyr_control	0.169 \pm 0.001	1.550	0.006
	Pyr_Rs	0.262 \pm 0.057		

^a*P*-value, the significance of the detoxification enzymes activity between Pyr_Control and Pyr_Rs were analyzed by Student's *t*-test using GraphPad 8.0 statistical software.

Table 3 Susceptibility to pyridaben after silencing *CYP4CL2* expression in laboratory strains and field populations of *P. citri*.

Origins	Mite	Treatments	Total number	Slope±SE	LC ₅₀ (95% CL) mg/L ^a	χ ² (df)	LCR ₅₀ (95% CL) ^b
Laboratory	Pyr_Control	ds <i>GFP</i>	502	2.717 ± 0.250	2.535 (2.261-2.901)	1.046 (5)	-
		ds <i>CYP4CL2</i>	431	2.964 ± 0.296	1.185 (1.039-1.322)	1.865 (4)	2.140 (1.799-2.545)
	Pyr_Rs	ds <i>GFP</i>	562	2.183 ± 0.210	1276.617(1134.408-1452.943)	4.445 (5)	-
		ds <i>CYP4CL2</i>	456	3.241 ± 0.331	637.595 (555.586-711.531)	3.513 (4)	2.002 (1.682-2.384)
Field	CQ_TN	ds <i>GFP</i>	381	2.082 ± 0.472	174.709 (134.830-261.562)	1.029 (4)	-
		ds <i>CYP4CL2</i>	459	1.596 ± 0.556	91.028 (25.559-129.269)	1.794 (3)	1.919 (1.076-3.424)
	CQ_WZ	ds <i>GFP</i>	517	1.589 ± 0.184	215.237 (180.123-269.557)	1.399 (6)	-
		ds <i>CYP4CL2</i>	527	1.402 ± 0.188	93.766 (73.103-113.524)	3.108 (5)	2.295 (1.712-3.076)

^aCL, confidence limits.

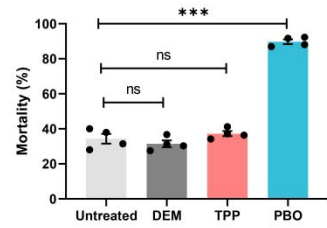
^bLCR₅₀, lethal concentration ratio at LC₅₀. If the 95% CL of LCR₅₀ >1, it indicated that ds*CYP4CL2* significantly reduced the resistance against pyridaben in *P. citri*.

Pyr_Control and Pyr_Rs, two laboratory strains were recombination inbred lines obtained from hybridization and pyridaben selection.

CQ_TN and CQ_WZ, two field populations were collected from citrus orchards in Tongnan, Chongqing municipality and Wanzhou,

Chongqing municipality.

Table of Contents graphic



Panonychus citri

Synergistic test

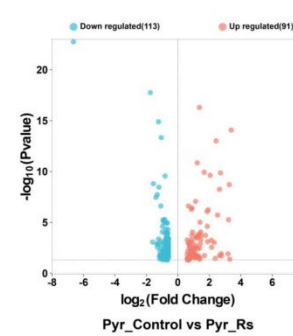
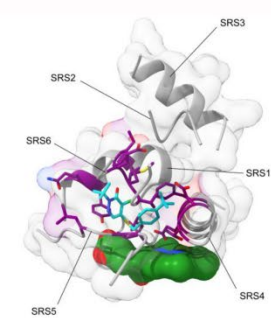
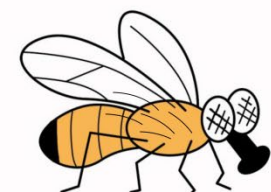
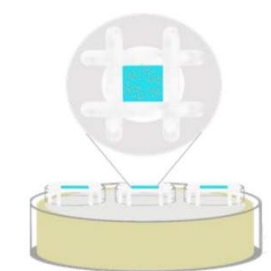
Cross-resistance

RNA-seq

dsCYP4CL2 feeding

Transgenic flies

Molecular docking



Based on the segregated pyridaben resistant and susceptible strains, this study systematically investigated the cross-resistance to eleven acaricides in *Panonychus citri* when the pyridaben resistance developed. We comparatively analyzed the detoxification enzymes activity (P450, CarEs and GSTs) in resistant and susceptible strains, and confirmed the effects of three synergists (DEM,

TPP and PBO) on the susceptibility of the mite to pyridaben. A upregulated P450 gene (*CYP4CL2*) was identified in resistant strain via RNA-seq. Furtherly, function verification of RNA interference-mediated and overexpression in transgenic flies demonstrated the important role of *CYP4CL2* in pyridaben resistance development. Molecular docking provided more evidences in the binding pattern between pyridaben and *CYP4CL2*.